



5G Communication with a Heterogeneous, Agile Mobile network in the Pyeongchang Winter Olympic Competition

Grant agreement n. 723247

Deliverable D3.5 mmWave backhauling & fronthauling platform

Date of Delivery:	5 June 2017
Editor:	Marko Pettissalo (Nokia)
Associate Editors:	
Authors:	Tommi Kallio (Nokia), Aki Korvala (Nokia) Juha Kestilä (Nokia), Harri Mustajärvi (Nokia), Giuseppe Destino (UOULU), Marko Leinonen (UOULU), Junhyeong Kim (ETRI), Heesang Chung (ETRI), Gosan Noh (ETRI), Bing Hui (ETRI), Ilgyu Kim (ETRI), Young-Min Choi (CL), Yongsoo Na (HFR), Sungmin Cho (SKT), Dongha Kim (SMRT)
Dissemination Level:	PU
Security:	Public
Status:	Final
Version:	V1.01
File Name:	5GChampion_D3_5
Work Package:	WP3



Title: Deliverable D3.5: mmWave backhauling & fronthauling platform

Date: 05-06-2017

Status: Final

Security: Public

Version: V1.01

Abstract

This deliverable provides description of integration of the key elements developed in the 5GCHAMPION project. There will be two different demonstration systems, one for EU and one for Korea. From the stationary EU test bed point of view, the key topic here is implementation study of proposed beamforming algorithm on physical demonstration platform for mmW wireless backhaul to be used in WP6. Korean high speed train testbed shows design and implementation of the baseband and radio units and those integration.

Index terms

5G, mmWave, backhaul link, algorithm, beamforming.



Title: Deliverable D3.5: mmWave backhauling & fronthauling platform
Date: 05-06-2017
Security: Public

Status: Final
Version: V1.01

Contents

1	Introduction	9
2	Key components of the EU mmWave transceiver platform.....	9
2.1	Overview of the demonstration platform	9
2.1.1	<i>The Antenna Unit:</i>	11
2.1.2	<i>The TRX Radio Unit</i>	19
2.1.3	<i>The BB Unit, Baseband Unit</i>	19
3	Beamforming control software	20
3.1	RSS acquisition	20
3.2	Beam adjustment	23
4	Integrating mmWave transceiver, proposed beamforming and demonstration platform.....	24
4.1	Available Interfaces and parameters from demonstration platform	24
4.2	RF i/f and Reference clock	25
4.3	Digital signals	25
4.4	Port for Captured IQ Data etc	26
5	Design, implementation, and testing of mmWave-based backhaul transceiver for high speed train	26
5.1	Baseband design	26
5.1.1	<i>Numerology and frame structure</i>	27
5.1.2	<i>Modulation and channel coding</i>	30
5.1.3	<i>Reference signal design</i>	32
5.1.4	<i>Baseband processing</i>	34
5.2	RF front-end design	36
5.2.1	<i>RF design parameters</i>	36
5.2.2	<i>RF design</i>	37
5.2.3	<i>Antenna design</i>	39
5.3	Testing procedures and preliminary results	40
5.3.1	<i>Indoor lab test</i>	40
5.3.2	<i>Subway field test</i>	42



Title: Deliverable D3.5: mmWave backhauling & fronthauling platform

Date: 05-06-2017

Status: Final

Security: Public

Version: V1.01

6 Conclusion.....44

References44



Title: Deliverable D3.5: mmWave backhauling & fronthauling platform

Date: 05-06-2017

Status: Final

Security: Public

Version: V1.01

List of Acronyms

3GPP	3 rd Generation Partnership Project
5G	5 th Generation
5GTN	5G Test network
AGC	automatic gain control
BB	Baseband
BRU	Backhaul Radio Unit
CA	Carrier aggregation
CC	Component carrier
C-RAN	Cloud radio access network
CRC	Cyclic redundancy check
dBi	decibel isotropic
DU	Digital unit
EIRP	Effective isotropic radiated power
EU	European union
GaN	Gallium nitride
GP	Guard period
HW	Hardware
IF	intermediate frequency
KPI	Key performance indicator
KR	Korea
LNA	low noise amplifier
LO	local oscillator
LoS	line-of-sight
MCS	Modulation coding scheme
MHN-E	Mobile Hotspot Network Enhancement
MIMO	Multiple-input-multiple-output
MME	Mobility Management Entity
MMIC	monolithic microwave integrated circuit
mmW	millimeter wave
MUX	Multiplexer
MWB	Mobile wireless backhaul
OFDM	Orthogonal frequency-division multiplexing
OIP	output intercept point
PA	Power amplifier
PCB	Printed circuit board
PoC	Proof of Concept
QAM	Quadrature amplitude modulation
QPSK	Quadrature Phase Shift Keying
RF-DFE	Radio Frequency Digital Frontend
RoF	Radio-over-Fiber
RSSI	Received signal strength indicator
RU	Radio unit
SDN	Software defined networking
SFBC	Spatial frequency block code
SNR	Signal-to-Noise Ratio
SPDT	Single point double throw
TBS	Transport block size



Title: Deliverable D3.5: mmWave backhauling & fronthauling platform

Date: 05-06-2017

Status: Final

Security: Public

Version: V1.01

TDD	Time Division Duplex
TE	Terminal equipment
UE	User equipment
WP	Work package



Table of Figures

Figure 1 5GCHAMPION EU mmW testbed building blocks.....	10
Figure 2 Functional split of different modules in the 5GCHAMPION EU mmW backhaul testbed	10
Figure 3 Logical Connection between Antenna Units and TRX Unit	12
Figure 4 Antenna Unit Control SW Architecture.....	13
Figure 5 RF SW state machine	14
Figure 6 Synchronization state machine	14
Figure 7 Timing diagram of TRU.....	15
Figure 8 TRU and RRU state machines.....	16
Figure 9 Timing simulation of the beamforming.....	16
Figure 10 Communication state machine.....	17
Figure 11 Developed Antenna Unit Mechanics enclosure	18
Figure 12 Antenna Unit boards and connectors.....	19
Figure 13 Logical BB functions.....	20
Figure 14 Beamformer state machine	20
Figure 15 Antenna Unit power measurement	20
Figure 16 RSS signal power and timing of power vector signals when the receiver changes the RF beamformer	22
Figure 17 Probability of misalignment	23
Figure 18 Beam Adjustment state machine	23
Figure 19 Timing diagram of the beam adjustment	24
Figure 20 TRX Radio Unit and Antenna Unit interface signals	25
Figure 21 System architecture of MHN-E.	27
Figure 22 Contiguous intra-band carrier aggregation	28
Figure 23 Frame structure of MHN-E system	28
Figure 24 Received SNR at mTE	29
Figure 25 Frame structure enabling CA, efficient neighbour cell search and fast handover. .	30
Figure 26 Channel coding processing for DCI, MI, HI, DL-SCH and UL-SCH	32
Figure 27 Mapping of downlink reference signal.....	33
Figure 28 Mapping of uplink reference signal	34
Figure 29 Uplink frequency estimation range.....	34
Figure 30 mNB/mDU MODEM architecture and interface to higher layer	34



Title: Deliverable D3.5: mmWave backhauling & fronthauling platform

Date: 05-06-2017

Status: Final

Security: Public

Version: V1.01

Figure 31 mTE MODEM architecture and interface to higher layer	35
Figure 32 Baseband processing of modulator	36
Figure 33 Block diagram of IF and LO part	38
Figure 34 Block diagram of mmWave part	38
Figure 35 TX antenna structure	39
Figure 36 RX antenna structure	39
Figure 37 Layout of MHN radio unit	40
Figure 38 Concept of indoor link test setup	41
Figure 39 Picture of test setup for indoor link	41
Figure 40 Peak data rates in diagnostic monitors	42
Figure 41 Seoul subway Line 8 path for a field trial	43
Figure 42 Picture of installed mRU	43
Figure 43 Measured performance of the MHN system in a field trial	44



Title:	Deliverable D3.5: mmWave backhauling & fronthauling platform	Status: Final
Date: 05-06-2017		
Security: Public		Version: V1.01

1 Introduction

EU mmW backhaul test bed i.e. demonstration platform is introduced at the high level and we describe how to integrate it with developed Antenna Unit discussed in 5GCHAMPION D3.1 [7]. Antenna Unit accommodates also proposed beam forming and/or beam switching algorithm from D3.2 [8].

Regarding the mmWave-based backhaul transceiver for high speed train, we describe the design and implementation of baseband and RF front-end. In addition, some preliminary test results are provided.

2 Key components of the EU mmWave transceiver platform

In this chapter, developed key components for the EU mmWave backhaul transceiver platform are introduced. The developed mmWave RF front-end and antenna design from 5GCHAMPION WP3 Task 3.1. will be introduced firstly, followed by proposed beamforming and/or switching functions developed in the Task 3.2. Third portion of this chapter will be high level description of the existing mmWave demonstration platform from Nokia.

2.1 Overview of the demonstration platform

The demonstration platform provides features and KPIs as listed in the previous deliverables D2.1 [9] and D2.2 [10]:

It comprises of three physical units; BBU, TRX Radio Unit and Antenna Unit. Two complete set of these systems are used for the mmW backhaul demonstration, pointing directly to each other as the typical wireless backhaul link application.

BBU unit is separated from TRX Radio Unit and Antenna Units and is connected to TRX Unit via optical cable. System includes two Antenna Units. In Figure 1 and Figure 2, the platform illustration and functional block illustrations are provided, respectively.



Title: Deliverable D3.5: mmWave backhauling & fronthauling platform

Date: 05-06-2017

Status: Final

Security: Public

Version: V1.01

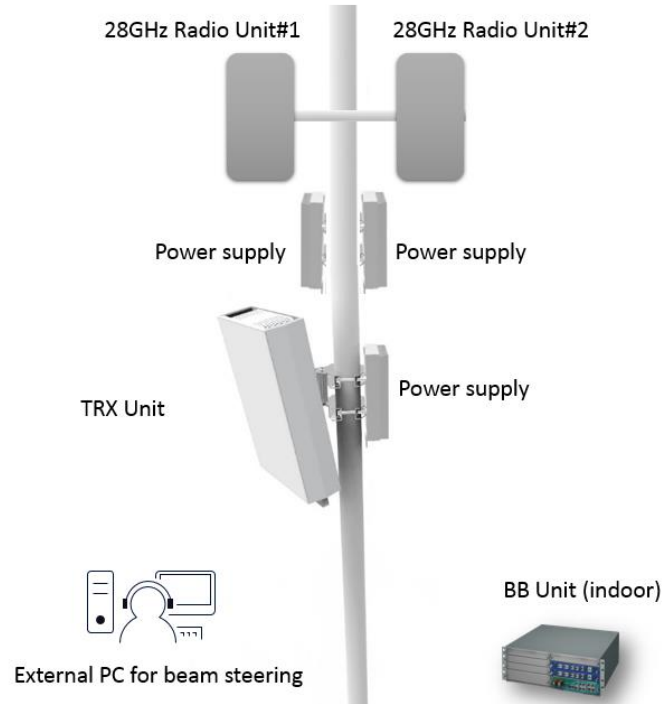


Figure 1 5GCHAMPION EU mmW testbed building blocks

Figure below show the key components, using green color to indicate the actual building blocks developed in the this project.

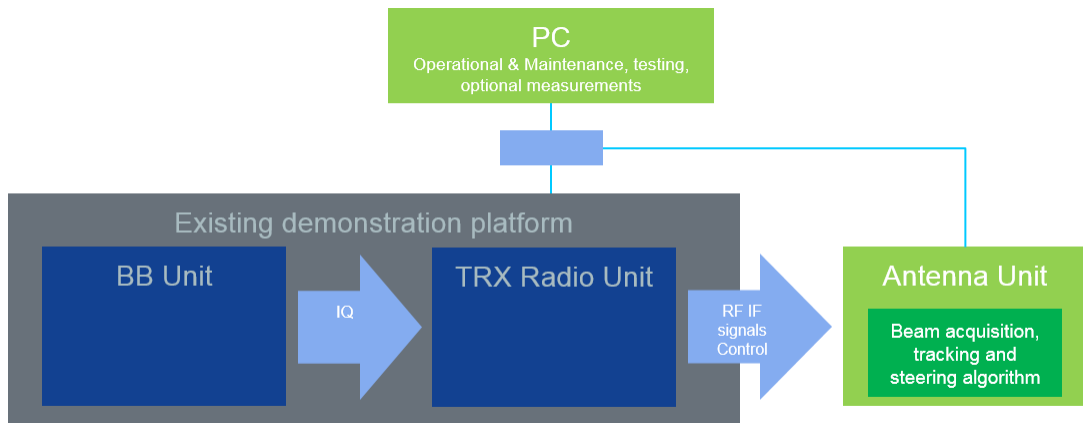


Figure 2 Functional split of different modules in the 5GCHAMPION EU mmW backhaul testbed



Title: Deliverable D3.5: mmWave backhauling & fronthauling platform
Date: 05-06-2017
Security: Public

Status: Final
Version: V1.01

The BB unit implements a LTE x5 type BB and numerology:

MIMO-OFDM
with 100MHz Carrier Component
up-to 64QAM modulation.
Multiple Carrier Components can be aggregated in the frequency domain, reaching an overall maximum bandwidth of 800 MHz

Operational frequency at 26.5-29.3 GHz, focus on 26.5 to 27.5 GHz used in the Olympics.

Table 1 Design goals for EU mmW backhaul testbed

Design Parameters	Values
Frequency	28 GHz
Bandwidth	up-to 800MHz
EIRP	up-to 60dBm
Modulation order	QPSK, 16QAM, 64QAM
Antenna configurations	2x2 MIMO
Maximum throughput of MWB (demonstration)	up-to 2.5Gbps

2.1.1 The Antenna Unit:

The antenna unit is illustrated in Figure 3 and comprises:

- An auxiliary board with an MCU. The MCU provides control functionalities of the RF components including, phase-shifters, RF-input attenuator, power amplifiers, carrier frequency oscillator, RSS measurements and input/output connectivity with external boards Phase-shift control,
- Two RF boards for dual polarization transmissions with RF beamforming capabilities
- Two planar phased array with 8x2 antennas built as 2x2 subarray

A detailed description of the physical interface with the TRX Unit as well as the inter unit interfaces are described in chapter 4.1. In Figure 3 we show the logical connections

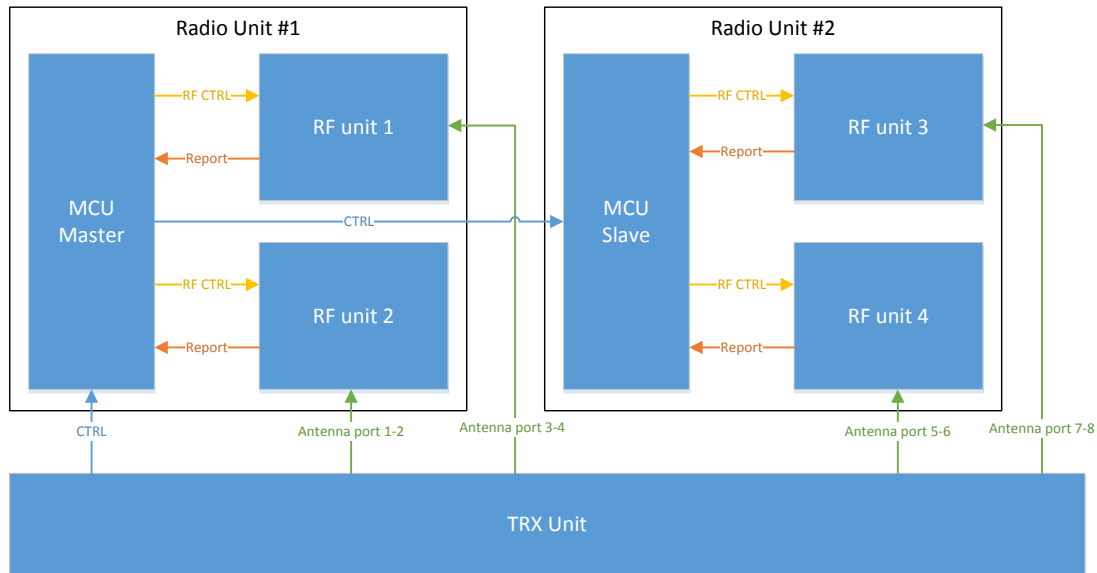


Figure 3 Logical Connection between Antenna Units and TRX Unit

The control signals from TRX Unit to MCU master includes timing and reference clock information. It is important to maintain the synchronization both at slot and sub-frame levels.

Each MCU controls two RF units independently. However, the alignment of the two RF with the TRX Unit is managed by the master MCU.

RF units can provide RF power report to the MCUs so as to perform AGC as well as BF alignment.



2.1.1.1 SW architecture

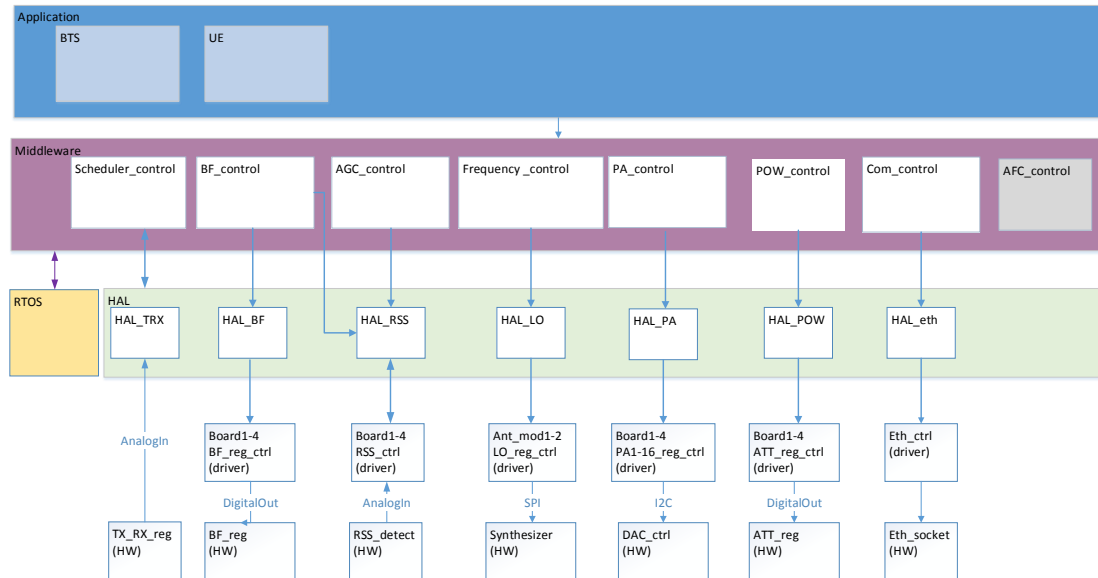


Figure 4 Antenna Unit Control SW Architecture

The SW architecture of the control software is illustrated in Figure 3: It consists of:

- **Application layer:** The BTS SW is the SW implemented in the TRU. It provides the high level control for DL signaling as well as DL data transmission. The UE SW is implemented in the RRU and provides the high level control of for DL signal power measurements as well as UL signaling.
- **Middleware:** The middleware comprises of all control processes, which will run simultaneously. The control processes are defined beamforming, AGC, frequency control, PA control, power control and communication with external units as PC or MCU.
- **Hardware abstraction layer:** The HAL is a library that allows middleware processes to command the HW with a level of abstraction (without knowing the HW implementation details). The functions will directly connect to low-level SWs (drivers).
- **Driver:** The drivers are HW specific and include procedures that operate directly on signals (input/output of the MCU).

2.1.1.2 SW functionalities

The high level description of the RF SW state machine is illustrated in Figure 5

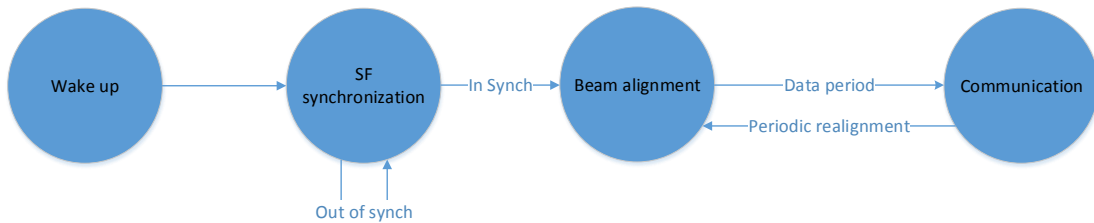


Figure 5 RF SW state machine

After the wake-up state, the RF unit hardware is ready to start the SF synchronization process, in which the TRU and RRU will align the slot counting.

The process will terminate when the RRU will acknowledge the time alignment and it is ready to start the beam alignment procedure.

The beam alignment procedure will follow the exhaustive search algorithm described in D3.4 [11] and it will terminate when both transmitter and receiver complete the beam sweep.

Finally, the TRU and RRU will proceed with the DL/UL data transmissions. The periodicity of the beam sweep will be defined based upon experiments.

2.1.1.2.1 Synchronization state

The synchronization state is a time-critical process that tackles the SF synchronization between TRU and RRU. In the TRU, this process is implemented with the state machine illustrated in Figure 6. It can be noticed that the DL control signal is transmitted for every SFP. Also, that the BF control is activated only at the occurrence of a PSS transmission.

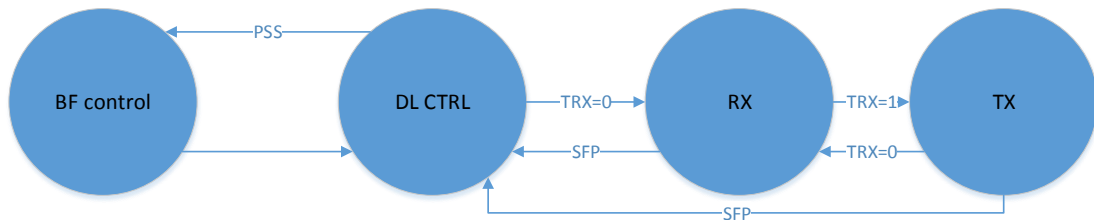
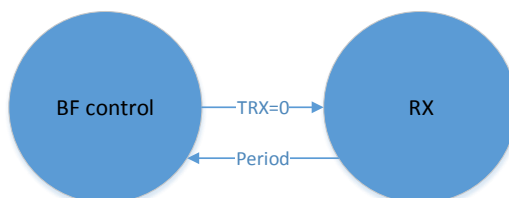


Figure 6 Synchronization state machine

In the RRU, the synchronization state is essentially a two-state process: BF control and RX. The RRU, in fact, will continuously search for the PSS signal from the TRU.



In the following figure we illustrate a simulation of the timing diagram for the TRU.

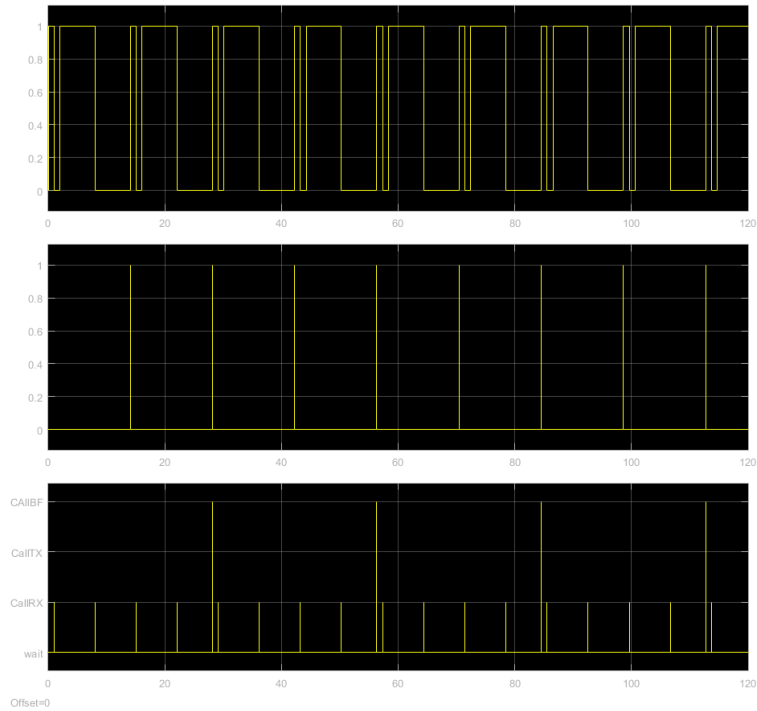


Figure 7 Timing diagram of TRU

In the top, a plot of the Tx/Rx signal is shown. The 0 level corresponds to UL mode and the 1 level to DL mode. The signal pattern follows the SF structure described in D2.1 [9].

The middle plot shows the start frame pulse (SFP) signal provided from the DFE. At the TRU, the SFP is used to call the BF control process (CallBF level in the bottom plot) which will prepare the RF beamformer logic for the next beam sweep.

A beam will be changed with the same periodicity of the PSS (in the figure, for instance, every two SF). After, the scheduler will change to RX state and command the RSS measurement process to measure the RX signal power.

At the RRU, the SFP will not be generated until the BB is able to detect the PSS sent from the TRU. In this case the CallBF and CallRX are generated with a predetermined periodicity.

2.1.1.2.2 **Beam alignment state**

The beam alignment process has the objective to align the TRU and RRU beams so as to maximize the SNR: The DL control signals are used as reference signals. The maximum number of reference signal transmissions will be determined with experiments.

The TRU and RRU state machines are illustrated in Figure 8, respectively.

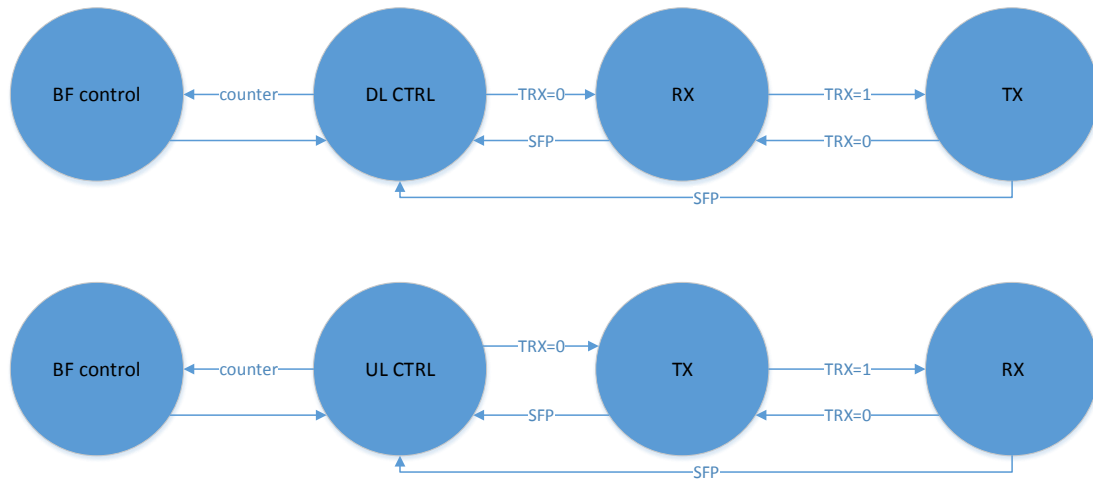


Figure 8 TRU and RRU state machines

It can be noticed that the beam alignment process is similar at TRU and RRU. However, the counter signal, which triggers the BF control, is different. In Figure 9, a simulation of the beamforming timing is illustrated. The left and right columns refer to the TRU and RRU timing, respectively.

The top plots show the Tx/Rx signal from the TRX Unit. The SFP signal is shown in the middle plots at left and right. This signal is aligned with the rising time of the DL control slot. The bottom plots indicate the trigger signals for the BF control and RX state. In this example, we can notice the different periodicity of the BF control trigger at the TRU and RRU.

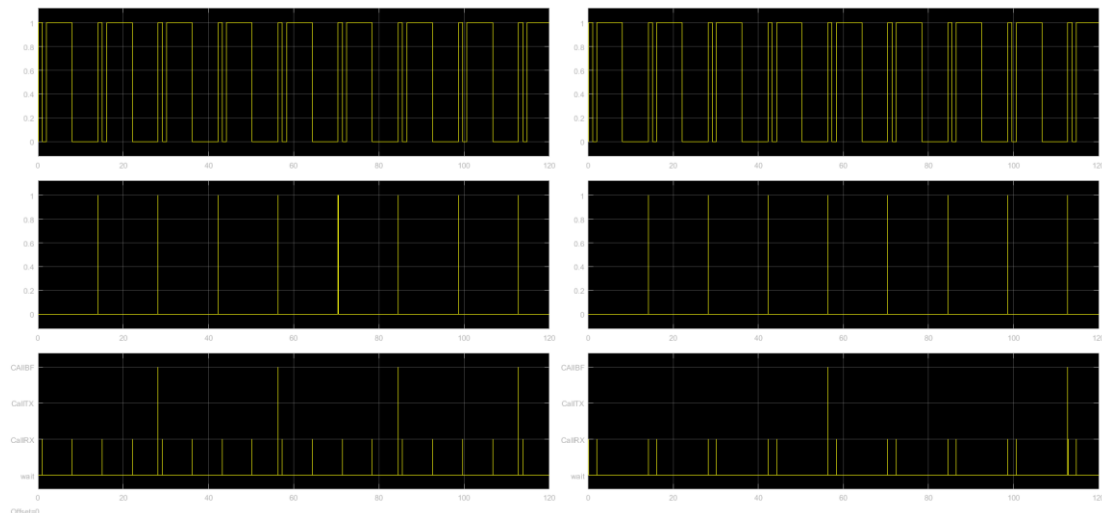


Figure 9 Timing simulation of the beamforming

2.1.1.2.3 Communication state

The information contained in this document is the property of the contractors. It cannot be reproduced or transmitted to thirds without the authorization of the contractors.



Title: Deliverable D3.5: mmWave backhauling & fronthauling platform

Date: 05-06-2017

Status: Final

Security: Public

Version: V1.01

The communication state is simply defined by two-state machine shown in Figure 10. No specific operations are performed.

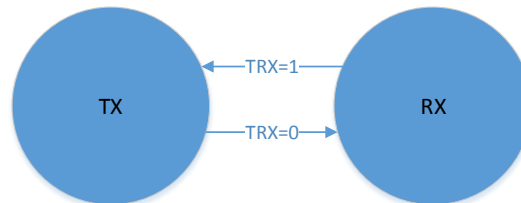


Figure 10 Communication state machine

2.1.1.3 Antenna Unit mechanics

Device main enclosure consist of milled aluminum frame and polymer based antenna cover, Figure 11. These main parts establish core mechanics with gaskets and PWB covers. Core mechanics function is to provide needed cooling capacity, grounding, and protection for PWB's. Antenna cover material and thickness is optimized taking account material availability.

Main Properties:

- Dimensions: (WxHxD) 400 x 570 x 80mm
- Environmental protection: IP 42

Additional parts (Outer enclosure, Fan frame, fan assembly, top/bottom caps, mounting bracket) will provide follow functions:

- Establish final outlook of antenna module
- Enables Forced cooling
- Provide needed grip for handling & installation
- Enables installation with tilting option.

Module top level layout

- RF and Control PWB's are separate and each have dedicated EMI covers.
- All interconnections inside antenna module are done via cables.



Title: Deliverable D3.5: mmWave backhauling & fronthauling platform

Date: 05-06-2017

Status: Final

Security: Public

Version: V1.01

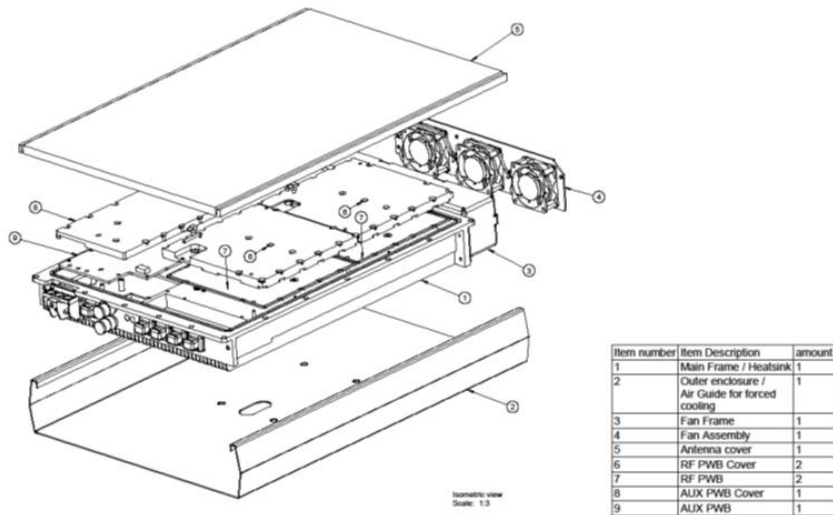
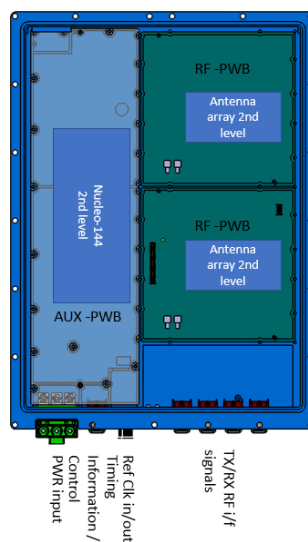


Figure 11 Developed Antenna Unit Mechanics enclosure

Antenna Unit boards mechanical layout and connections are shown in Figure 12

- An auxiliary board with an MCU.
- Two RF boards for with planar phased array antennas



The information contained in this document is the property of the contractors. It cannot be reproduced or transmitted to thirds without the authorization of the contractors.



Title:	Deliverable D3.5: mmWave backhauling & fronthauling platform	Status:	Final
Date:	05-06-2017	Version:	V1.01
Security:	Public		

Figure 12 Antenna Unit boards and connectors

2.1.1.3.1 Thermal Solution

Forced cooling is selected as it enables greatly smaller unit size than fanless, especially when cooling is single sided (antenna on the other side)

- All electronics are thermally coupled to main heat sink
- Thermal vias are used for components on opposite side of the board than heat sink

Three 60x60x25 mm fans are used to pull air through the unit

- A visual cover is forming a duct around the fins and preventing air by passing the fins
- Fans are PWM controllable to keep unit in more constant temperature and reducing acoustics noise

2.1.2 The TRX Radio Unit

The TRX Radio Unit includes following functionalities: Interface to BBU via optical cable, Complex Numerically Controlled Oscillator (NCOs), Interpolation/decimation filter, RF impairment correction, ADC/DAC, Wideband IQ up/down, Synthesizer and LO.

The key functions enabling the integration are the Rx/Tx RF intermediate frequency signals and control and timing signals towards the developed Antenna Unit. These are discussed in more details in the Chapter 4.

In addition, there are fan and power supply modules for the TRX Radio Unit.

2.1.3 The BB Unit, Baseband Unit

Figure 13 show the logical architecture of BBU. It consists of several sub-modules including encoder and decoder, downlink modulator, and uplink demodulator. Additionally, the BBU includes the front-end for pre-coding and FFT in addition to cell searcher. BBU interfaces to the corresponding L1 controller. Additionally, the BBU also provides I/Q samples and timing control signaling for the TRX Unit and both Antenna Units.

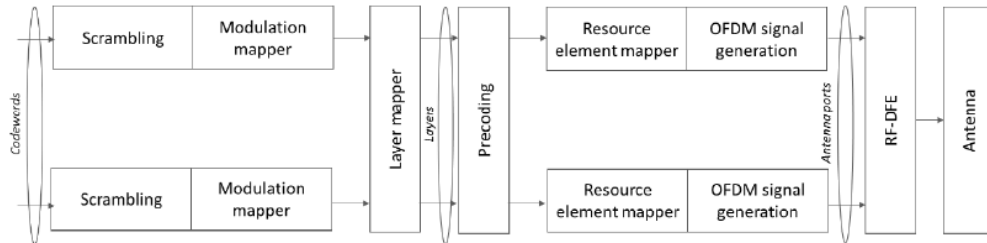


Figure 13 Logical BB functions

3 Beamforming control software

The beamformer software is implemented with the state machine shown in Figure 14. The RSS values with their time index are used to compute the beam direction with maximum SNR. Following, at the HAL, the direction is converted into beamforming weights. Then, phase-shifter registers are loaded and latched to the phase-shifters upon a trigger pulse.



Figure 14 Beamformer state machine

3.1 RSS acquisition

In the RF domain, RF-based RSS measurements are applied for the initial beam acquisition and searching. RSSI measurement is made in the Antenna Unit for all RF paths. Measurement is handled in the MCU of the Antenna Unit. In the Antenna Unit radio, power measurement system as indicated in Figure 15.

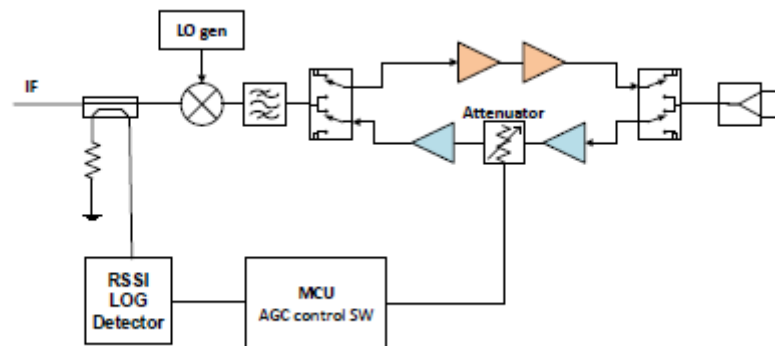


Figure 15 Antenna Unit power measurement



Title: Deliverable D3.5: mmWave backhauling & fronthauling platform

Date: 05-06-2017

Status: Final

Security: Public

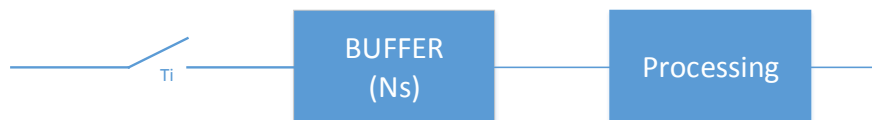
Version: V1.01

From a mathematical perspective the RSS measurements are modelled as follows. Let $y(t)$ be the continuous IF received signal. The output of the power log-detector is the instantaneous power $s(t)$ given by

$$s(t) = 10 \log_{10} \left(\frac{1}{T_d} \int_t^{t+T_d} \|y(t)\|^2 dt \right) \quad (1)$$

where T_d is the integration time, tunable via a capacitor.

At the MCU, an ADC is used to generate discrete samples of the power signal. The sampling frequency of the RSS signal is denoted by T_i and it is controlled by the AGC control SW. The samples are then processed and the result value is then used as RSS sample.



In [5] it was investigated the impact these two parameters on the probability of misalignment. In the following we shortly summarize the outcome.

Figure 16 shows a realization of the power signal vector and the resulting average. In Figure 16, we show a time sequence of power vector signals obtained when the receiver periodically changes the RF beamformer. The locations (sample index) of the peaks relate to arrival of the reference signal, whereas the magnitudes depend on the transmission power and the total equivalent" channel gain, which includes transmit and received array gains. The location of the maximum peak is used for the selection of the best transmit-receive beamformer pair.

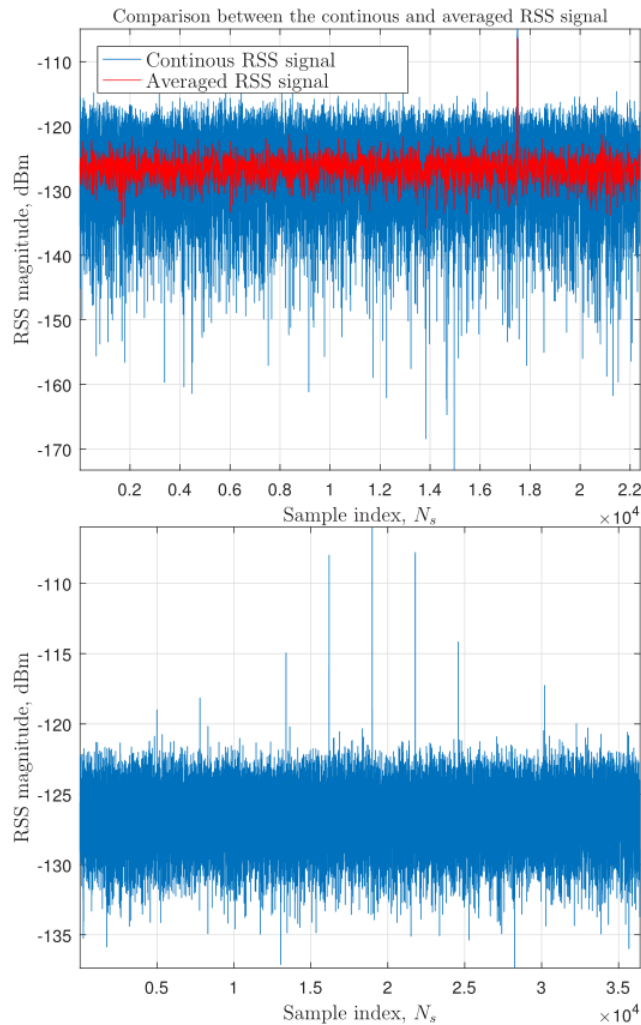


Figure 16 RSS signal power and timing of power vector signals when the receiver changes the RF beamformer

Figure 17 shows the probability of misalignment for a test scenario with TRU and RRU equipped of ULA with 8 elements and 11dBi gain per element (D2.1) [9]. The maximum achievable SNR is 50dB and it refers to the SNR achieved when TRU and RRU beams are perfectly aligned. The beam search is exhaustive search and beams are steered by δ_s degree at each step. The beam sweep covers a sector ± 30 degree. The TRU and RRU are time synchronized by means of 1-pulse-per-second (1-PPS) signal, however, the radio frames at the transmitter and receiver are not. The periodicity of the reference signal is 10 ms.

First, by comparing the results obtained with the same δ_s , we can observe that the shorter T_i , the lower the probability of misalignment is.

This is easy to understand as, for a given buffer size N_s , the higher the sampling frequency of the RSS signal, the more accurate the RSS calculation is. However, there is an increase of the number of signaling for ADC conversion.



Second, we observe that for a given T_i , there exists a range buffer size values that can minimize the probability of misalignment. Our intuition is that both the mean and the span of this optimal range depends on the ratio symbol and periodicity time. More specifically, the larger the ratio, the bigger the mean and the span are as more samples can be accumulated within the duration of the reference signal.

Third, we notice that by increasing the step-size δ_s , the lower the probability of misalignment is. However, by increasing δ_s beams are going to be more and more a part from each other leaving sub-sectors with low SNR. In light of the above, our approach for beam alignment is to use relatively wide δ_s steps to guarantee coverage, large T_i and small buffer size.

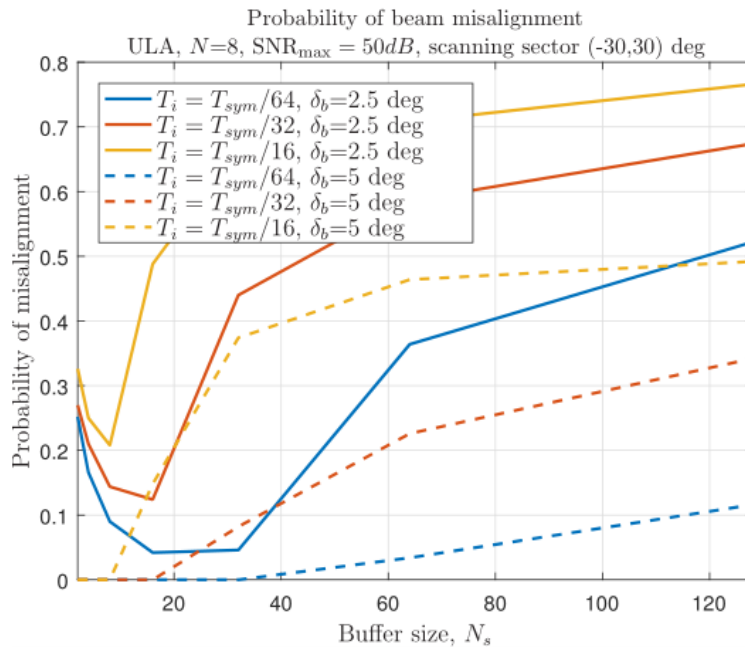


Figure 17 Probability of misalignment

3.2 Beam adjustment

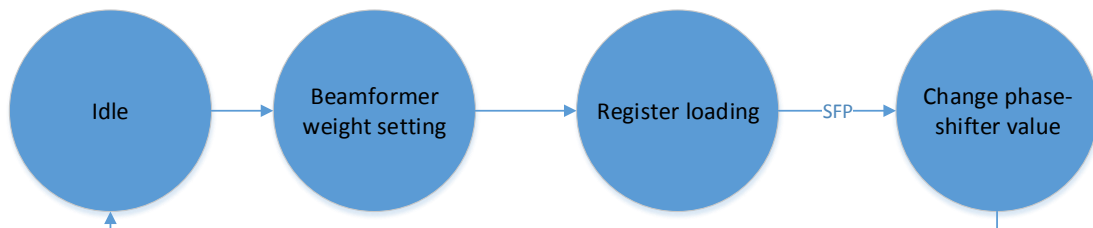


Figure 18 Beam Adjustment state machine

The beam adjustment procedure is implemented based on the state machine described in Figure 18. The weights are computed with the constraint that phase-shifters have finite resolution (11.25 degree). Following, the phase-values are converted into binary values are loaded to the phase-shifter register buffer (shadow-register). The latching signal is given by the SFP.



Figure 19 shows the time-diagram of the beam adjustment phase. Top-plot shows the SFP. The BF control is triggered after a predefined number of SFPs. The second plot shows, in fact, only one trigger for the BF control. The third and fourth plots shows how the beamforming weight setting, register loading and latching operations are scheduled. In the example, the time spent in the beamforming setting state is intentionally long in order to show that some computation delays can be afforded. The loading of the shadow register immediately follows the beamforming setting and, finally, the latching to the phase shift values is synchronized with the SFP.

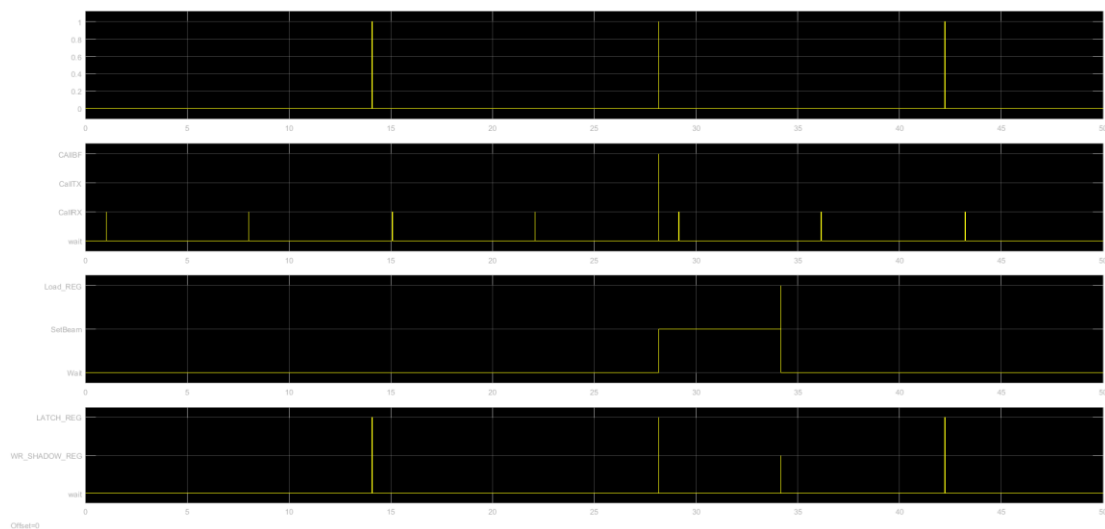


Figure 19 Timing diagram of the beam adjustment

4 Integrating mmWave transceiver, proposed beamforming and demonstration platform

4.1 Available Interfaces and parameters from demonstration platform

The key interface signal for integrating Antenna Units to existing demonstration platform is from TRX Radio Unit; RF signals for Tx and Rx, digital control signals for timing and Reference Clock.

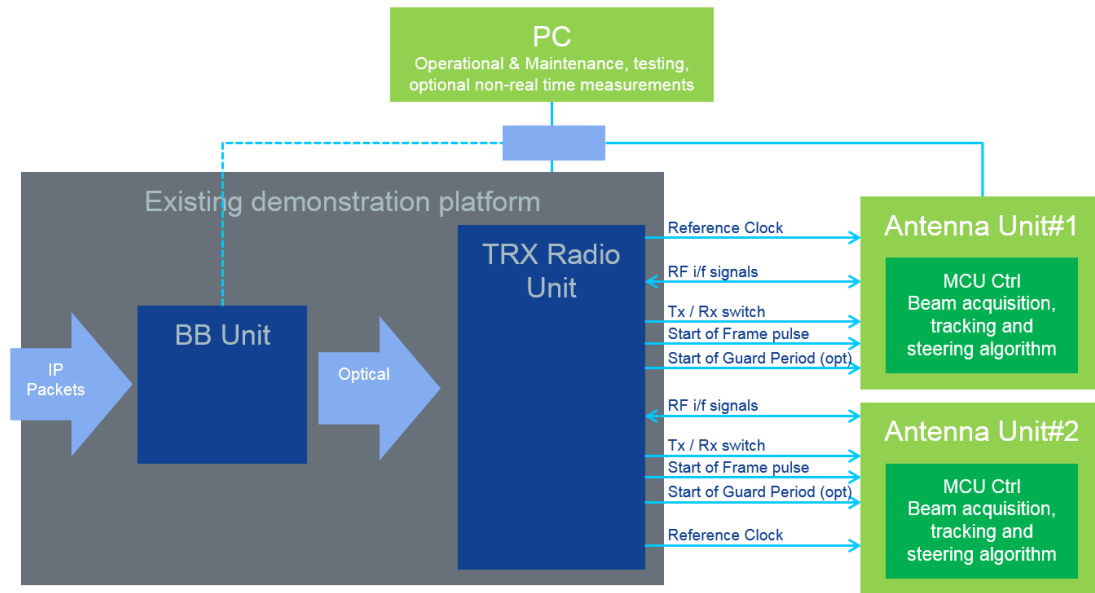


Figure 20 TRX Radio Unit and Antenna Unit interface signals

4.2 RF i/f and Reference clock

Table 2 RF Interface signal between TRX Radio Unit and Antenna Unit

	Design Parameters	Values
RF i/f	Frequency	few GHz
RF i/f	Bandwidth	400 / 800 MHz
Ref Clk	Frequency	230MHz

4.3 Digital signals

Digital control signals from the TRX Radio Unit related to beamforming and control timing are:

- Tx / Rx switch, indicating if there the ongoing OFDM symbol is meant to be Tx or Rx
- A pulse indicating start of the 10ms air frame.
- Optional guard period indicator i.e. giving a pulse when guard period between OFDM symbols starts.



Title: Deliverable D3.5: mmWave backhauling & fronthauling platform
Date: 05-06-2017
Security: Public
Status: Final
Version: V1.01

These signals are routed to both Antenna Units as differential digital signals. Also, some level of timing adjustment for the each signal could be expected for fine tuning of the mmW backhaul demonstration system and integration.

Table 3 Digital Interface signals between TRX Radio Unit and Antenna Units

	Design Parameters	Values
Digital Control and timing	Tx/Rx switch	LVDS
	Start of Air Frame	LVDS
	Start of Guard Period	LVDS

4.4 Port for Captured IQ Data etc

In the TRX Radio Unit, there is allocated internal memory for capturing I/Q samples, that is possible to download via Operational and Maintenance Port. It's usability for the 5GCHAMPION project is under planning.

5 Design, implementation, and testing of mmWave-based backhaul transceiver for high speed train

5.1 Baseband design

In this section, the baseband design of mobile hotspot network enhancement (MHN-E) system is addressed. The mmWave-based backhaul transceiver of the MHN-E system is designed to provide a broadband mobile wireless backhaul (MWB) for high-speed trains running at speeds of up to 500km/h, and the design goal of the MHN-E system is summarized in Table 4.

Table 4 Design goal of MHN-E system

Design Parameters	Values
Frequency	25.5 GHz
Bandwidth	1 GHz
EIRP	36 dBm
Mobility support	Up to 500 km/h

The information contained in this document is the property of the contractors. It cannot be reproduced or transmitted to thirds without the authorization of the contractors.



Title: Deliverable D3.5: mmWave backhauling & fronthauling platform

Date: 05-06-2017

Status: Final

Security: Public

Version: V1.01

Modulation order	QPSK, 16QAM, 64QAM, 256QAM
Antenna configurations	2x2 SFMF 2x2 MIMO
Maximum throughput of MWB (simulation)	10Gbps
Maximum throughput of MWB (demonstration)	2.5Gbps

The system architecture of the MHN-E system basically originate in the hierarchical two-hop network, which, as illustrated in Figure 21, consists of MWB links outside using millimeter-wave and onboard access links. Since this network concept has several well-known advantages [2], it has already been applied to many commercialized railway communication systems [3], and is also being considered as one of the potential deployment scenarios by both 3GPP and IEEE 802 [4].

In the MHN network, MHN digital unit (mDU) and MHN radio unit (mRU) are separated from each other and interconnected via optical fiber, which forms an efficient cloud radio access network (C-RAN). Each individual mRU with its corresponding mDU functions as a base station, hence has a unique cell ID different from others. As illustrated in Figure 21, the mRUs are deployed along the trackside, and two mRUs installed in the same location transmit sharp beams pointing to opposite directions. As a result, MHN terminal equipments (mTEs) mounted on top of both head and rear sides of the train could receive independent signals sent from mRUs of different sites simultaneously. Each mTE behaves like a single user connected to onboard access link providing mobile Internet service to user equipments (UEs) carried by passengers in the train.

In this section, we focus on the baseband design of the MWB link in the MHN-E system.

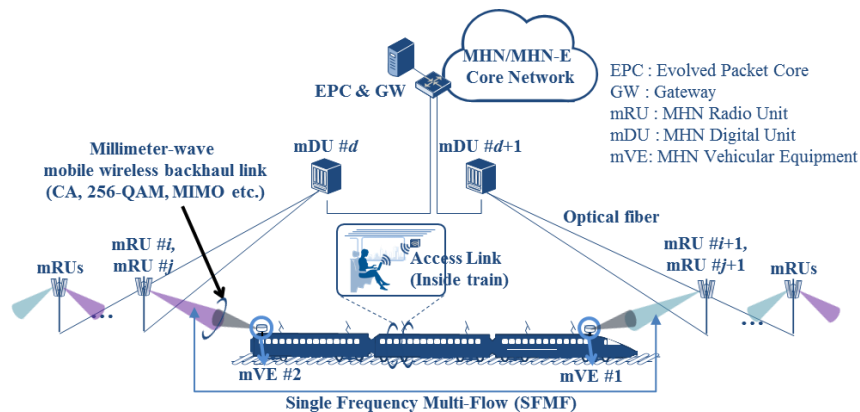


Figure 21 System architecture of MHN-E.

5.1.1 Numerology and frame structure

One of the main features included in the MHN-E specification is a frame structure enabling carrier aggregation (CA), efficient neighbor cell search and high-performance handover as shown in Figure 22. Each aggregated carrier, generally referred to as a component carrier (CC), has a bandwidth of 125MHz, and orthogonal frequency division multiplexing (OFDM) parameters of which are basically identical to that of the MHN [3]. The MHN-E allows the aggregation of a maximum of eight CCs to attain a total transmission bandwidth of up to 1GHz.



Additionally, it is required that at least two CCs should be supported as mandatory and the different number of CCs, 2~8, can be configured depending on mTE capability.

Each configured CC in the MHN-E system employs OFDM for both uplink (UL) and downlink (DL) transmissions. In the testing and final demonstration, it will only support time-division duplex (TDD) as uplink-downlink duplexing. Considering that data traffic in high-speed scenarios is largely asymmetric in nature, where downloads typically accounts for most of the traffic, the DL is prioritized rather than UL in this case. In this regard, we focus on TDD for MHN-E. Like other cellular systems, as shown in Figure 23, TDD of MHN-E is able to offer dynamic resource allocation where time durations are changed as required.

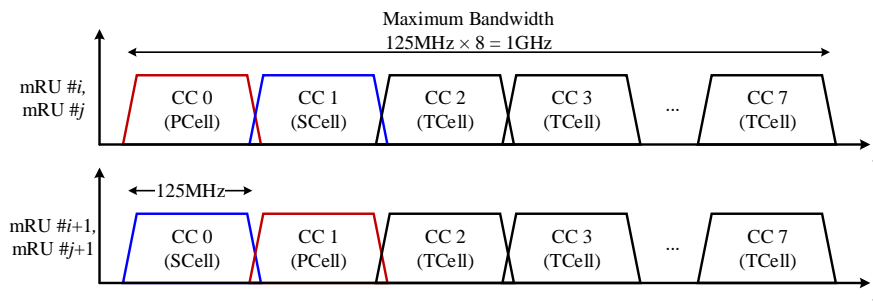


Figure 22 Contiguous intra-band carrier aggregation

Figure 23 shows the TDD frame structure of the system. A subframe has 8 slots and each slot is 250-us long. Each slot contains 40 OFDM symbols. One symbol is 6.25-us long which is the sum of the reciprocal of a subcarrier spacing of 180 kHz (5.56 us) and a cyclic prefix length of 0.69 us. The second slot in each subframe of 2ms, *l*-th slot (*l*=1,9,17,25,33), is a special slot, which consists of downlink pilot time slot (DwPTS), guard period (GP), and uplink pilot time slot (UpPTS). Figure 23 also shows three different UL-DL configuration supported in MHN-E, and their corresponding ratios of DL to UL.

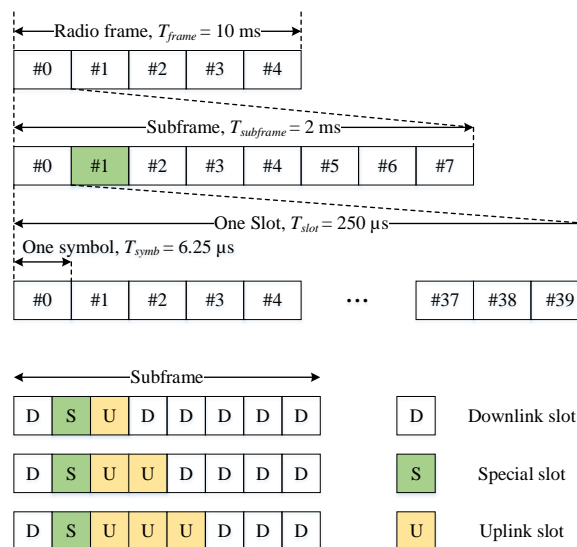


Figure 23 Frame structure of MHN-E system



Title: Deliverable D3.5: mmWave backhauling & fronthauling platform

Date: 05-06-2017

Status: Final

Security: Public

Version: V1.01

Table 5 gives the details of numerology for the MHN-E system.

Table 5 Numerology for MHN-E system

Parameters	Values
Subcarrier spacing	180 kHz
Sampling clock rate (MHz)	184.32
OFDM symbol duration, no CP (us)	5.56
CP duration (us)	0.69
CP overhead (%)	12.4
Number of symbols per TTI	40
TTI duration (ms)	0.25
Frame duration (ms)	10
Number of RBs in frequency domain	50
Number of subcarriers per RB	12
FFT size	1024

Due to the characteristics of received signal strength at mTE as shown in Figure 24 where the SNR received from serving mRU is much larger than that received from target mRU most of the time and drastically drops in a very short time, it is highly difficult to obtain cell information and timing synchronization of a target cell prior to handover. This is the main reason why three different cell types are defined in the system, which are primary cell (PCell), secondary cell (SCell), and tertiary cell (TCell) as shown in Figure 25. Each CC can be configured by one of the cell types. The first and second CCs are configured by either PCell or SCell depending on the location of mRU and the remaining CCs are configured by TCell.

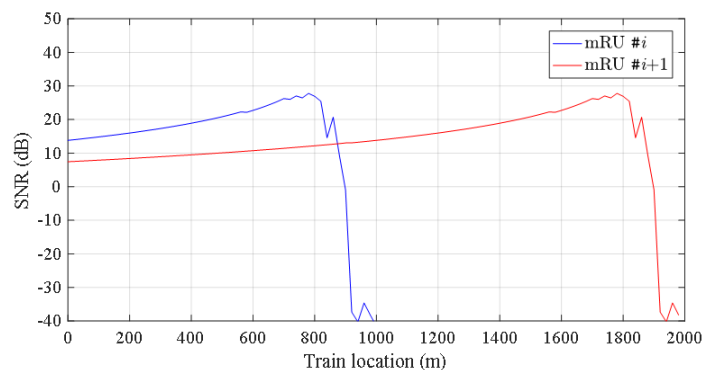


Figure 24 Received SNR at mTE

As illustrated in Figure 25, the PCell is not only responsible for sending data and control channels, but also for sending MHN synchronization signal and cell information through MHN

The information contained in this document is the property of the contractors. It cannot be reproduced or transmitted to thirds without the authorization of the contractors.



broadcast channel (M-BCH). The SCell and TCell, on the other hand, only send data and control information. The main difference between the two is that the SCell vacates the resource location where MHN broadcast channel (M-BCH) or synchronization signal is transmitted in the PCell to detect target cell signal without interference from serving cell.

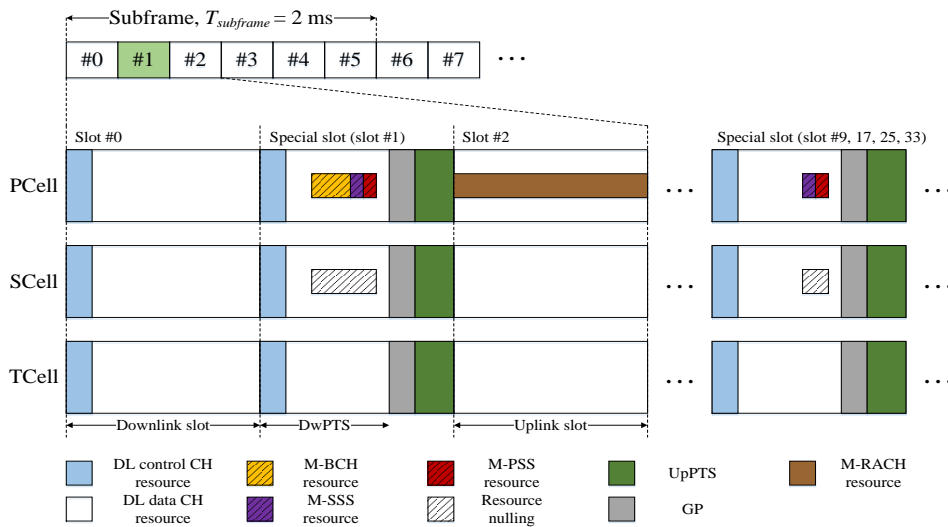


Figure 25 Frame structure enabling CA, efficient neighbour cell search and fast handover.

Additionally, MHN random access channel (M-RACH), mainly used to get access to the network and obtain timing alignment information to synchronize uplink transmissions, is designed to be transmitted only in the PCell. Since in most cases, there is no train/mTE or only one train/mTE in a cell, there is almost little possibility of collision among the requests coming from multiple mTEs. So, the design of M-RACH could be a contention-free-based, and its procedure can be significantly simplified as compared with that of Cellular systems.

5.1.2 Modulation and channel coding

This section describes modulation schemes channel codings. Table 6 shows the table of modulation and coding schemes (MCSs) for downlink transmission, and Table 7 show the transport block size (TBS) table for usage of both uplink and downlink.

Table 6 MCS table for downlink

MCS Index	modulation	coding rate x 1024	efficiency	Code Rate
0	2	120	0.2344	0.11718750
1	2	157	0.3057	0.15332031
2	2	193	0.3770	0.18847656
3	2	321	0.6270	0.31347656
4	2	449	0.8770	0.43847656
5	2	603	1.1768	0.58886719
6	4	301	1.1768	0.29394531
7	4	378	1.4766	0.36914063
8	4	434	1.6954	0.42382813
9	4	490	1.9141	0.47851563



Title: Deliverable D3.5: mmWave backhauling & fronthauling platform
Date: 05-06-2017
Security: Public
Status: Final
Version: V1.01

10	4	553	2.1602	0.54003906
11	4	616	2.4063	0.60156250
12	4	658	2.5684	0.64257813
13	6	438	2.5684	0.42773438
14	6	466	2.7305	0.45507813
15	6	517	3.0264	0.50488281
16	6	567	3.3223	0.55371094
17	6	616	3.6123	0.60156250
18	6	666	3.9023	0.65039063
19	6	719	4.2129	0.70214844
20	6	772	4.5234	0.75390625
21	6	822	4.8193	0.80273438
22	6	873	5.1152	0.85253906
23	6	910	5.3350	0.88867188
24	8	683	5.3350	0.66699219
25	8	711	5.5547	0.69433594
26	8	797	6.2266	0.77832031
27	8	885	6.9141	0.86425781
28	Implicit TBS signaling with QPSK			
29	Implicit TBS signaling with 16QAM			
30	Implicit TBS signaling with 64QAM			
31	Implicit TBS signaling with 256QAM			

Table 7 TBS table

I_{PRB}	N_{PRB}									
	1	2	3	4	5	6	7	8	9	10
0	56	176	272	368	472	568	664	760	856	952
1	72	232	360	488	616	744	872	1000	1128	1256
2	104	296	448	600	760	920	1096	1274	1454	1634
3	184	384	584	792	1000	1192	1416	1608	1832	2024
4	232	480	728	984	1224	1480	1736	1992	2216	2472
5	240	504	760	1032	1288	1544	1800	2088	2344	2600
6	288	600	904	1224	1512	1832	2152	2472	2792	3112
7	344	712	1064	1448	1800	2152	2536	2920	3304	3624
8	408	840	1256	1704	2152	2536	2984	3432	3880	4264
9	472	952	1448	1960	2472	2920	3432	3944	4392	4904
10	536	1096	1640	2216	2728	3304	3880	4456	4968	5544
11	600	1224	1832	2472	3048	3688	4328	4904	5544	6128
12	680	1384	2088	2792	3560	4264	4968	5672	6336	7048
13	776	1576	2408	3176	4008	4776	5608	6360	7160	7968
14	872	1800	2664	3624	4520	5416	6280	7184	8096	9000
15	984	1992	2984	4008	5032	6056	7000	8016	9024	10032
16	1064	2152	3240	4264	5352	6408	7488	8568	9640	10720
17	1128	2280	3432	4584	5736	6808	7952	9104	10248	11392
18	1256	2536	3816	5032	6288	7560	8832	10104	11376	12624
19	1352	2792	4136	5544	6904	8304	9696	11088	12464	13856
20	1480	2984	4520	6056	7504	9024	10536	12056	13544	15064
21	1608	3240	4904	6480	8120	9760	11400	13016	14656	16296
22	1736	3496	5288	7008	8776	10544	12288	14056	15832	17600
23	1864	3752	5672	7528	9424	11328	13200	15104	17000	18880
24	1992	4008	6056	8016	10040	12064	14064	16088	18112	20112
25	2152	4264	6376	8520	10672	12792	14944	17088	19216	21360
26	2216	4456	6648	8888	11128	13344	15584	17816	20032	22272
27	2280	4648	6928	9256	11592	13904	16232	18544	20880	23208
28	2600	5224	7776	10392	12976	15592	18208	20800	23416	26008
29	2856	5800	8640	11544	14424	17328	20208	23112	25992	28896
I_{PRB}	N_{PRB}									
	11	12	13	14	15	16	17	18	19	20
0	1064	1160	1256	1352	1448	1544	1640	1736	1832	1928
1	1384	1512	1640	1768	1896	2024	2152	2280	2408	2536

I_{PRB}	N_{PRB}									
	41	42	43	44	45	46	47	48	49	50
28	80712	83328	85920	88528	91144	93736	96352	98944	101560	104152
29	89640	92520	95424	98304	101208	104088	106992	109896	112776	115680
I_{PRB}	N_{PRB}									
	41	42	43	44	45	46	47	48	49	50
0	4008	4136	4200	4328	4392	4520	4584	4712	4776	4904
1	5224	5352	5480	5608	5736	5928	6056	6128	6240	6368
2	6416	6576	6736	6896	7056	7208	7368	7528	7688	7848
3	8368	8576	8784	8984	9192	9400	9608	9808	10016	10224
4	10288	10536	10792	11048	11296	11552	11808	12056	12288	12536
5	10728	10984	11248	11512	11776	12040	12280	12544	12808	13072
6	12648	12960	13272	13584	13896	14208	14520	14824	15136	15448
7	15008	15376	15744	16112	16480	16848	17216	17584	17952	18320
8	17592	18024	18432	18864	19296	19728	20160	20592	21024	21456
9	20128	20624	21112	21608	22104	22600	23088	23584	24080	24544
10	22720	23272	23832	24384	24920	25480	26032	26592	27152	27704
11	25280	25904	26520	27144	27760	28384	29000	29624	30240	30840
12	29048	29760	30472	31184	31872	32584	33296	34008	34720	35432
13	32792	33600	34400	35200	36008	36784	37592	38392	39200	40000
14	37008	37912	38824	39728	40632	41544	42448	43336	44240	45144
15	41240	42256	43240	44248	45264	46272	47280	48280	49280	50288
16	44048	45128	46200	47280	48360	49416	50496	51576	52656	53736
17	46800	47952	49072	50216	51368	52512	53656	54800	55928	57072
18	51928	53200	54472	55720	56992	58264	59536	60808	62056	63328
19	56944	58344	59736	61128	62504	63896	65296	66688	68084	69456
20	61864	63384	64896	66416	67904	69424	70936	72456	73944	75464
21	66912	68528	70168	71800	73424	75056	76696	78336	79952	81592
22	72232	73976	75752	77520	79288	81032	82800	84568	86320	88088
23	77560	79456	81336	83232	85136	87008	88912	90808	92688	94584
24	82576	84600	86600	88624	90648	92648	94664	96688	98688	100712
25	87704	89848	91976	94120	96272	98392	100544	102688	104816	106960
26	91432	93648	95888	98104	100344	102584	104800	107040	109280	111496
27	95240	97576	99888	102216	104528	106864	109192	111504	113832	116168
28	106768	109384	111968	114584	117176	119792	122384	125000	127616	130208

This section also describes coding procedures which are used for more than one transport channel or control information type. The usage of channel coding scheme and coding rate for TrCHs is defined in Table 8 and, the usage of channel coding scheme and coding rate for control information is summarized in Table 9. The code rate of Turbo coding applied to TrCH of both UL-SCH and DL-SCH is 1/3. A tail biting convolutional code with constraint length 7 and coding rate 1/3 is used for control information including DCI, MI, HI, UCI.

The information contained in this document is the property of the contractors. It cannot be reproduced or transmitted to thirds without the authorization of the contractors.



Table 8 Usage of channel coding scheme and coding rate for TrCHs

TrCH	Coding scheme	Coding rate
UL-SCH	Turbo coding	1/3
DL-SCH		

Table 9 Usage of channel coding scheme and coding rate for control information

Control Information	Coding scheme	Coding rate
DCI	Tail biting convolutional coding	1/3
MI	Tail biting convolutional coding	1/3
HI	Repetition code	1/6
UCI	Block code	variable
	Tail biting convolutional coding	1/3

Figure 26 shows the channel coding procedure for each case.

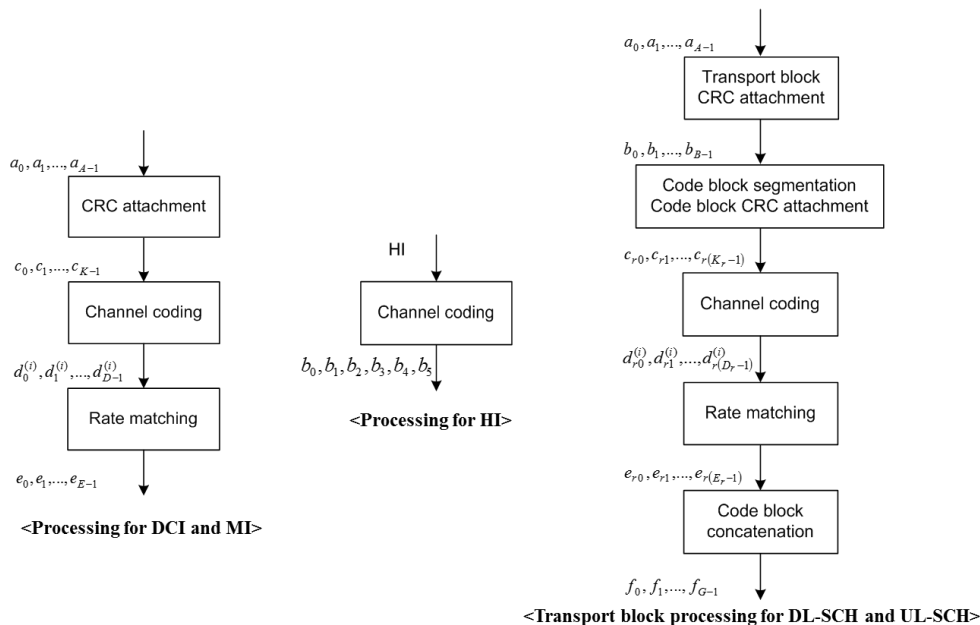


Figure 26 Channel coding processing for DCI, MI, HI, DL-SCH and UL-SCH

5.1.3 Reference signal design

Figure 27 **Error! Reference source not found.** shows the mapping of downlink reference signals, which is cell-specific. The downlink reference signal is designed to use a lattice type allocation, and the allocation of the reference signals is for a total of two antenna ports. The



period in the time domain is four symbols, and the period in the frequency domain is six subcarriers.

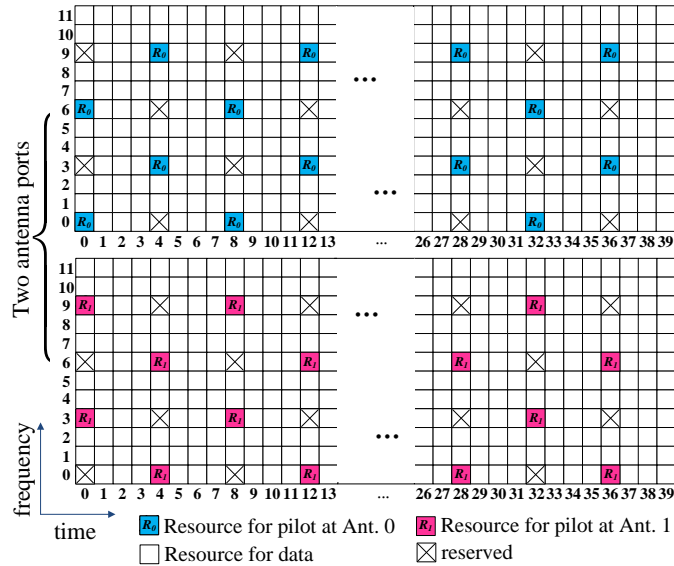


Figure 27 Mapping of downlink reference signal

Figure 28 shows the mapping of uplink reference signals, which is mTE-specific. The percentage of the symbols of the reference signals is 12.5%. In typical cellular systems like LTE, symbols for uplink reference signals are generally deployed in a regular interval. However, since in the uplink transmission, frequency offset caused by Doppler is twice larger than that of downlink, a new reference signal design is required. Therefore, the uplink reference signal in the MHN-E system is designed in a different way, where the first two reference signals in the time domain are arranged closer than the others in order to resolve the Doppler problem in a HST channel.

As shown in Figure 29, the frequency offset f_1 (blue line) that can be estimated by 2nd and 5th reference signals in time domain is ± 26.67 kHz while the frequency offset f_2 (red line) that can be estimated by 5th, 14th, 23th and 32th reference signals in time domain pilots is ± 8.89 kHz. The final frequency offset f_o can be calculated as follows:

$$f_o = \begin{cases} (f_1 + f_2) / 2 & \text{if } |f_1| \leq 8.89 \text{ kHz} \\ (f_1 + f_2) / 2 + 8.89 \text{ kHz} & \text{if } f_1 > 8.89 \text{ kHz} \\ (f_1 + f_2) / 2 - 8.89 \text{ kHz} & \text{if } f_1 < -8.89 \text{ kHz} \end{cases}$$

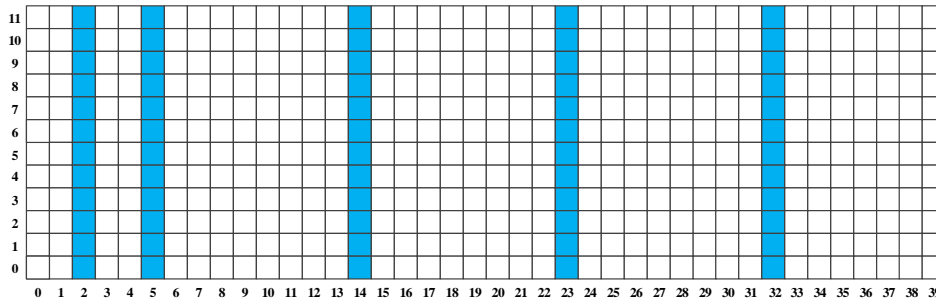


Figure 28 Mapping of uplink reference signal

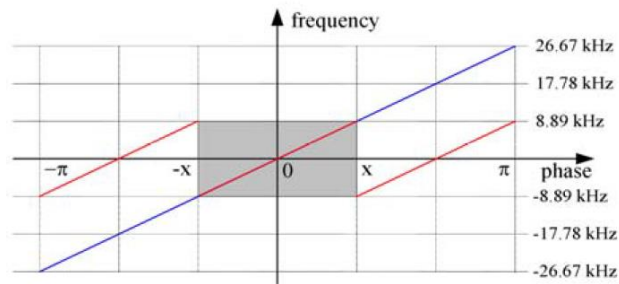


Figure 29 Uplink frequency estimation range

5.1.4 Baseband processing

Figure 30 and Figure 31 show the architecture of mDU and mTE MODEMs. The mDU MODEM consists of several sub-modules including TrCH encoder, TrCH decoder, downlink modulator, and uplink demodulator. Similarly, the mTE MODEM consists of several sub-modules including TrCH encoder, TrCH decoder, uplink modulator, and downlink demodulator. Additionally, the mTE MODEM includes the front-end controller and cell searcher. For both mDU and mTE MODEMs, interfaces to the corresponding L1 controller are configured. Additionally, the mTE MODEM also provides control signalling for the antenna module.

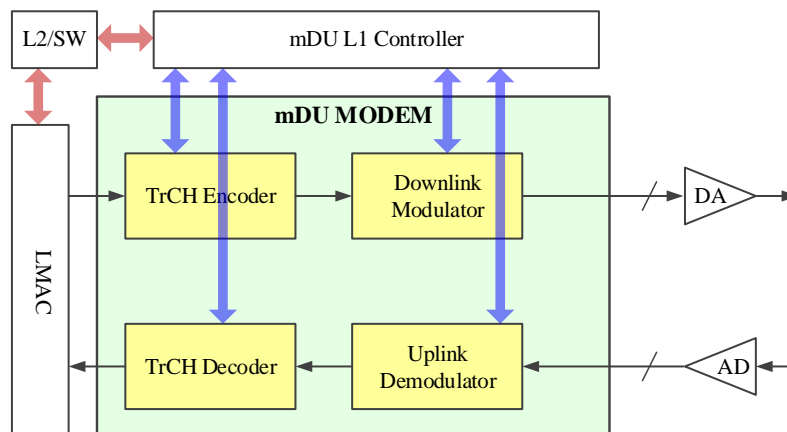


Figure 30 mNB/mDU MODEM architecture and interface to higher layer

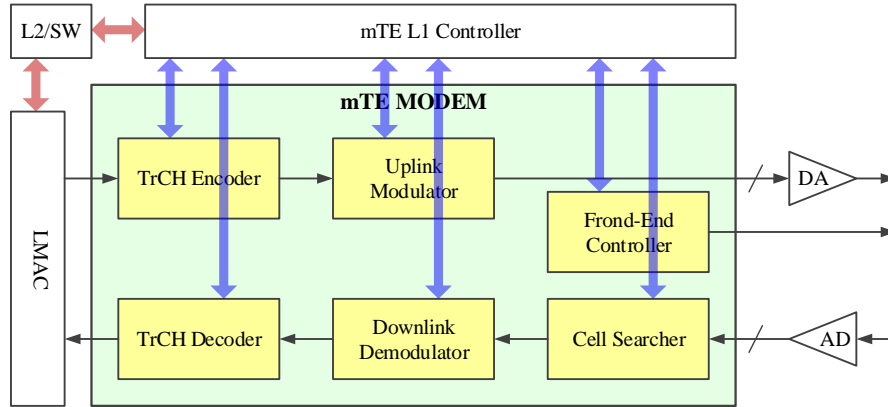


Figure 31 mTE MODEM architecture and interface to higher layer

Figure 32 shows the baseband processing of the modulator in mDU and mTE MODEMs. First, the data stream from the high layer is divided into code blocks during block segmentation. Cyclic redundancy check (CRC) bits are then appended to the code block so that the receiver can detect transmission errors using a CRC check. Next, depending on the type of source (see subsection 5.1.2), the bit stream is encoded accordingly before being scrambled. The basic code rate used in the Turbo coding block is 1/3, although the precise code rates vary depending on the modulation and coding scheme (MCS) selected and the number of usable resource blocks. Bit-wise scrambling is then applied to achieve time diversity by randomizing the bit streams. A modulation mapper then transforms the scrambled bits into a series of complex symbols. Four modulation formats are available in the downlink transmission: QPSK, 16QAM, 64QAM and 256QAM while 256QAM is not supported in the uplink transmission. A layer mapper is used to map the modulated symbols to one or two layers, depending on the transmission mode. A single-antenna scheme only supports one layer, and precoding scheme for spatial frequency block codes (SFBC) and spatial multiplexing are used for two layers. The precoding operation for transmit diversity is defined for two antenna ports, and given by

$$\begin{bmatrix} y^{(0)}(2i) \\ y^{(1)}(2i) \\ y^{(0)}(2i+1) \\ y^{(1)}(2i+1) \end{bmatrix} = \frac{1}{\sqrt{2}} \begin{bmatrix} 1 & 0 & j & 0 \\ 0 & -1 & 0 & j \\ 0 & 1 & 0 & j \\ 1 & 0 & -j & 0 \end{bmatrix} \begin{bmatrix} \text{Re}(x^{(0)}(i)) \\ \text{Re}(x^{(1)}(i)) \\ \text{Im}(x^{(0)}(i)) \\ \text{Im}(x^{(1)}(i)) \end{bmatrix},$$

and the precoding for spatial multiplexing is defined by

$$\begin{bmatrix} y^{(0)}(i) \\ \vdots \\ y^{(p-1)}(i) \end{bmatrix} = W(i) \begin{bmatrix} x^{(0)}(i) \\ \vdots \\ x^{(v-1)}(i) \end{bmatrix},$$

where the precoding matrix $W(i)$ is of size $p \times v$ and given by



$$W(i) = \frac{1}{\sqrt{2}} \begin{bmatrix} 1 & 0 \\ 0 & 1 \end{bmatrix}.$$

The layer mapping and precoding blocks are followed by one or two resource element mappers. After resource mapping, the outputs are transformed into time domain data through an inverse discrete Fourier transform. Then, the data is combined using a cyclic prefix and sent to the antennas.

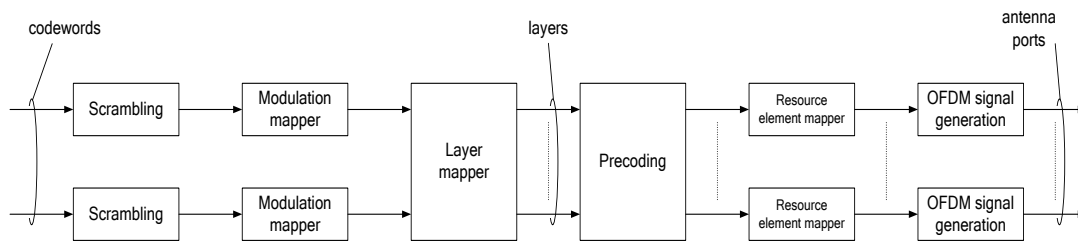


Figure 32 Baseband processing of modulator

5.2 RF front-end design

5.2.1 RF design parameters

The mobile hotspot network (MHN) system will be implemented step-wise over two years by 5G CHAMPION's Korea partners. This subsection describes the MHN system aiming at the first year's goal and corresponding RF design requirements. Table 10 summarizes the MHN system requirements.

Table 10 MHN system requirement

Item	Specification
Carrier frequency	24 – 26.5 GHz
Frequency bandwidth	500 MHz
Number of component carrier	4 x 125 MHz
Duplex Mode	TDD (Time Domain Duplex)
Data Throughput	Downlink Link (DL): 1.25 Gbps Uplink Link (UL): 180 Mbps
Transmission Mode	DL: TX & RX diversity UL: Receive diversity
RF transmit & receive path	2T2R (Base station), 1T2R (Terminal equipment)
Connection between DU & RU	Radio over fiber
Coverage	>300m (curved path), >500m (straight path)



Title: Deliverable D3.5: mmWave backhauling & fronthauling platform

Date: 05-06-2017

Status: Final

Security: Public

Version: V1.01

The RF designs for the MHN system should comply with the specification aforementioned. The RF transmit (TX) and receive (RX) path are 2TX & 2RX for a base station and 1TX & 2RX for a terminal equipment. One option among many is making two components including a TRX (transmit-receive) module and a RX module. Two TRX modules are used for a 2T2R base station, and one TRX and RX module are used for a 1T2R terminal equipment. Table 11 describes TRX module parameters and ranges. When it comes to the RX module, the same table should be applied except the TX parameters.

Table 11 TRX Module Parameter

	Parameter	Range	Remarks
Common	Operating frequency	25.1056 ~ 25.5376GHz	
	Bandwidth	430MHz	without guard band
	DIF frequency	705.6~1137.6MHz	
	TDD switching time	< 5usec	
	TRX isolation	> 55dB	
TX	Output power	> +17dBm	P1dB : 27dBm
	Gain	> 37dB	
	Gain flatness	± 2.0dB	
	TX spurious	< -40dBc	Leakage
	TX DIF input	-20dBm	Single-ended
	TX EVM	< 3%	64QAM
RX	Noise figure	< 8dB	
	Input level	-20dBm ~ -61dBm	
	Gain	> 51dB	Max. gain at -35dBm input RX fixed attenuation
	Gain flatness	± 2.0dB	
	Gain control	≥ 0.5/31.5dB , ≥15dB	
	DIF output	-10dBm	

5.2.2 RF design

The RF design consists of three parts: intermediate frequency (IF), local oscillator (LO) and mmWave part as shown in Figure 33 and Figure 34. IF and mmWave part have two paths for transmit and receive, respectively. They are corresponding to a transmit antenna and receive antenna, respectively. The two paths are switched in the time domain by SPDT (Single Point Double Throw) switches. The output of IF is up-converted by a mixer with LO into mmWave frequencies. The frequency ranges for IF inputs are represented as 705.6-1137.6 MHz. The input power from a baseband transmitter is set to -20dBm and the output power from the IF is



Title: Deliverable D3.5: mmWave backhauling & fronthauling platform

Date: 05-06-2017

Status: Final

Security: Public

Version: V1.01

set to -10dBm. These values are specified in the TRX module parameters. The devices for digital attenuation and temperature compensations are also represented in the figure.

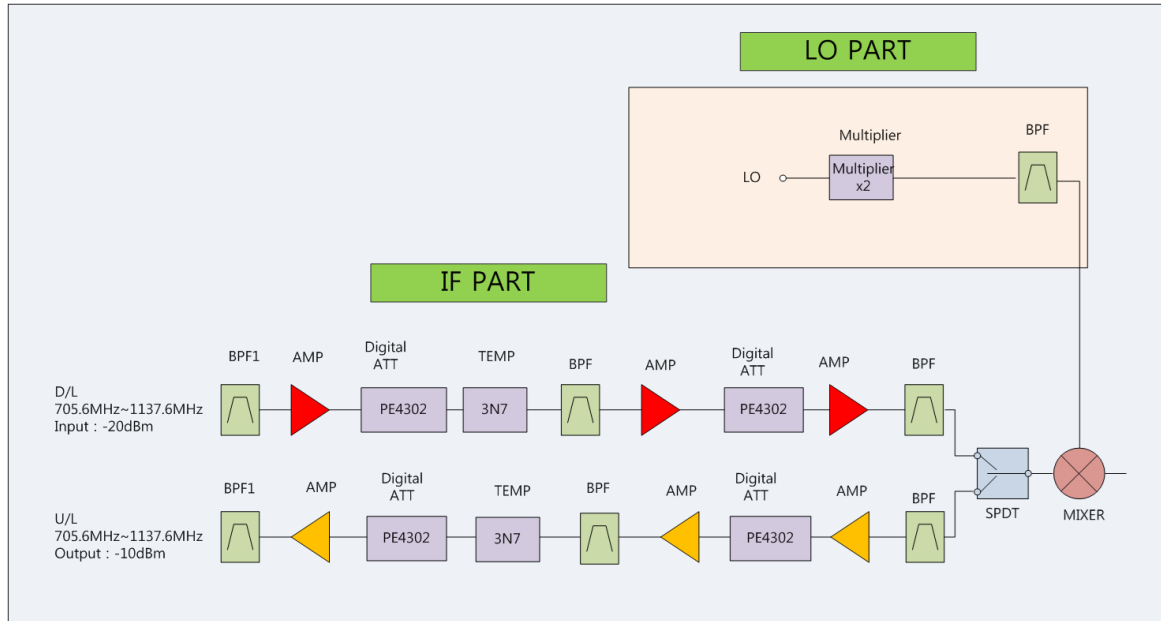


Figure 33 Block diagram of IF and LO part

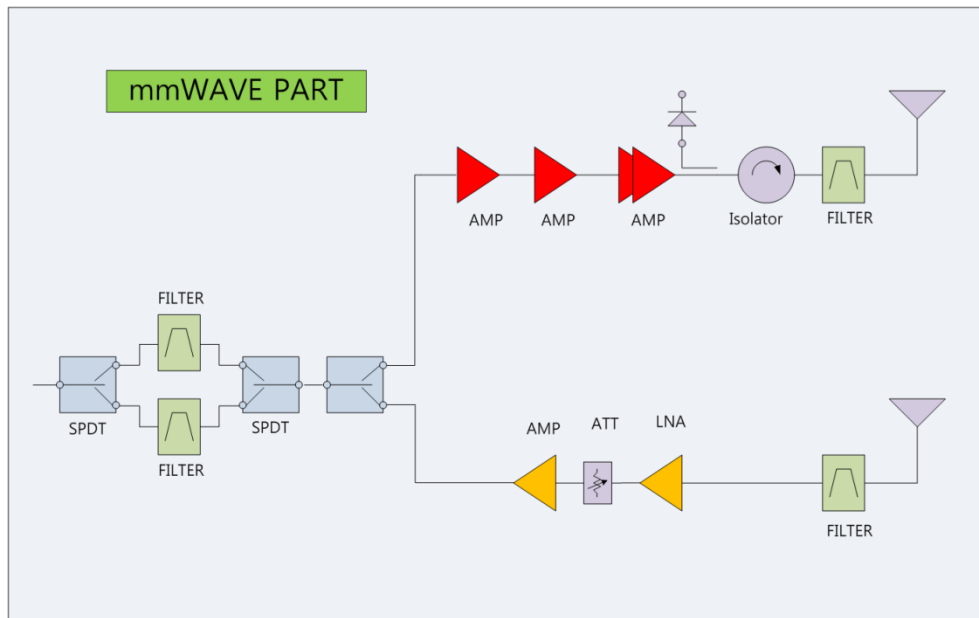


Figure 34 Block diagram of mmWave part

The information contained in this document is the property of the contractors. It cannot be reproduced or transmitted to thirds without the authorization of the contractors.



5.2.3 Antenna design

Antennas for the MHN system have 19-dBi beamforming gain for the transmission and 22-dBi gain for the reception. Since the transmission should meet the regulatory output power in terms of EIRP (Equivalent Isotropic Radiated Power), the maximum output power plus the beamforming gain is less than 36 dBi. On the other hand, the reception needs to have a slightly larger beamforming gain to achieve the coverage requirement in the Table 10. The structures of TX and RX antennas are shown in Figure 35 and Figure 36, respectively. Details on dimension is not described, but TX antenna is surely smaller than RX antenna in size due to the different beamforming gains.

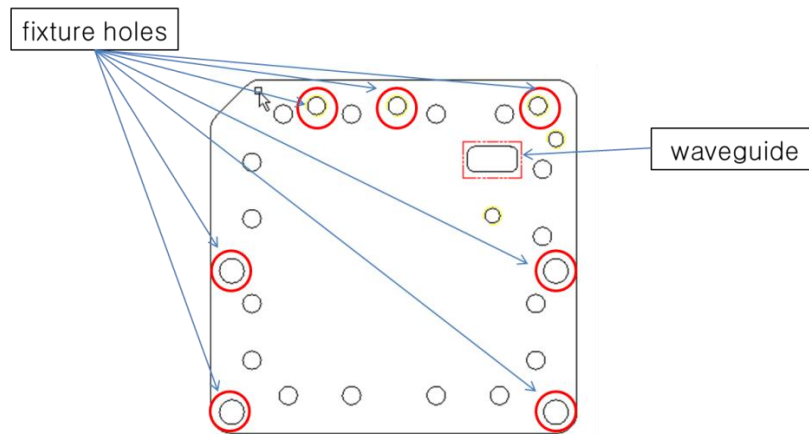


Figure 35 TX antenna structure

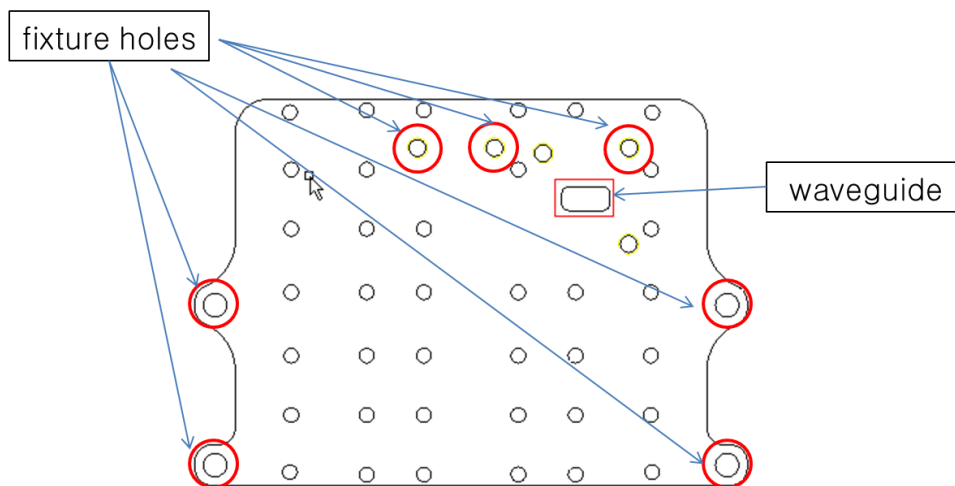


Figure 36 RX antenna structure

Figure 37 shows the layout of the MHN radio unit that includes two TRX modules and 2T2R antennas. A power supply module, local oscillator module and radio-over-fiber (RoF) interface module are included. The RoF interface is used to connect between the radio unit and corresponding baseband processing unit. The length of fiber between the two units is up to 5

The information contained in this document is the property of the contractors. It cannot be reproduced or transmitted to thirds without the authorization of the contractors.



Title: Deliverable D3.5: mmWave backhauling & fronthauling platform

Date: 05-06-2017

Status: Final

Security: Public

Version: V1.01

km. The beamformers used in the radio units are all for fixed beam. Since the main applications of the MHN system are for high-speed or subway trains and their route are predetermined, the fixed beamformers can cover all the routes by appropriate cell configurations considering curved and straight paths.

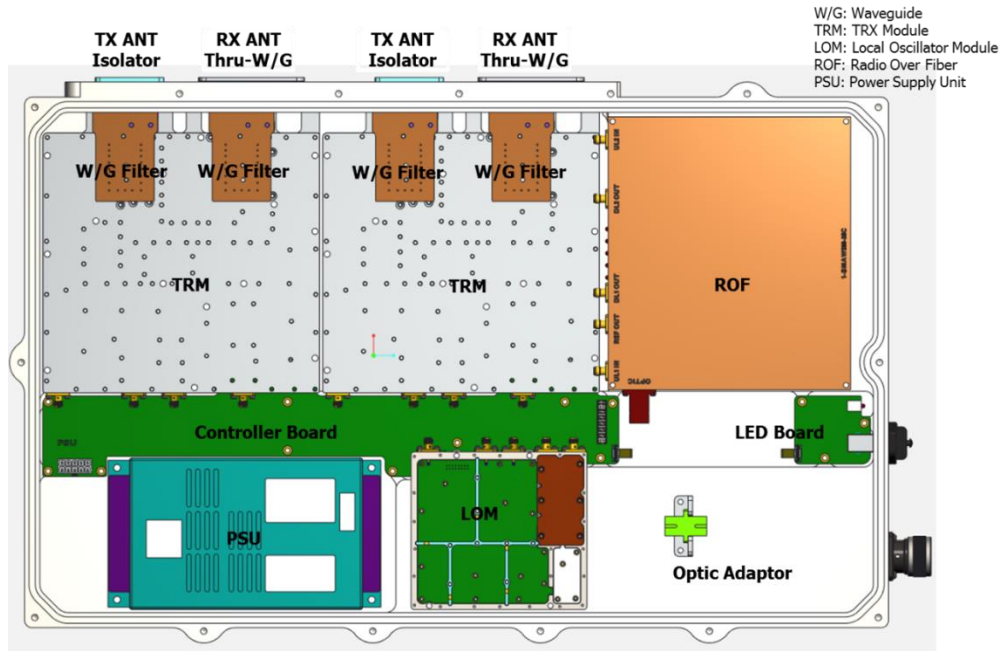


Figure 37 Layout of MHN radio unit

5.3 Testing procedures and preliminary results

5.3.1 Indoor lab test

Functionalities of the MHN system are primarily tested under an indoor environment. A test setup is shown in Figure 38. An mNB consist of an mDU (Digital Unit) and an mRU (Radio Unit). An mTE includes a baseband part and radio part in a module. In the figure, higher layer protocol stacks such as MAC, RLC, PDCP, RRC and NAS are represented, but they are not mandatory in a physical layer link test. The setup is for maximum downlink capacity of 1.25 Gbps. For 2.5 Gbps of downlink capacity, we use two links as in Figure 39. The figure shows two sets of the test link depicted in Figure 38. One important point is that the two links are using the same carrier frequency. Though they have the same frequency, the interference to the neighbor link is not so big to deteriorate each link performance since they adopt directional beams with narrow beam widths. Figure 40 shows two displays representing diagnostic monitors for each link, respectively. Each peak data rate is larger than 1.25 Gbps so that the aggregated data rate is larger than 2.5 Gbps.

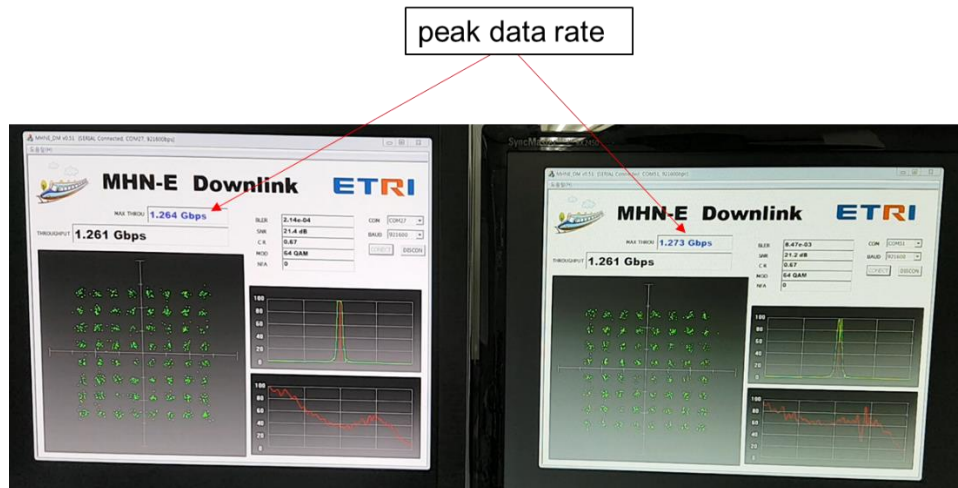


Figure 40 Peak data rates in diagnostic monitors

5.3.2 Subway field test

Real environments for the subway or high-speed trains are different from the indoor environment in many ways. First of all, the trains run under various channel environments such as the tunnels, rural, urban, viaduct, stations, mountains, etc. Therefore, it is meaningful to demonstrate the functionalities of the MHN system in the real world. The tunnel among many environments is very challenging since it represents strong and fast fading channel characteristics.

In this regard, the MHN system has been tested in the running subway trains of Seoul subway Line 8. Figure 41 shows a train path of Seoul subway Line 8 where the MHN systems was tested. There are three stations, Jamsil, Seokchon and Songpa from left to right in the figure. Four mRUs were installed between the Jamsil st. and Seokchon St. to cover the curved path. An mRU was installed near the Songpa St. for the straight path. The locations of the five radio units were determined by a wave propagation test using mmWave-based MHN prototypes before this field trial. The specification and characteristics of the used equipment are explained in the earlier subsections. Figure 42 illustrates a picture of an mRU installed on the wall of the tunnel along the train route.



Title: Deliverable D3.5: mmWave backhauling & fronthauling platform

Date: 05-06-2017

Status: Final

Security: Public

Version: V1.01

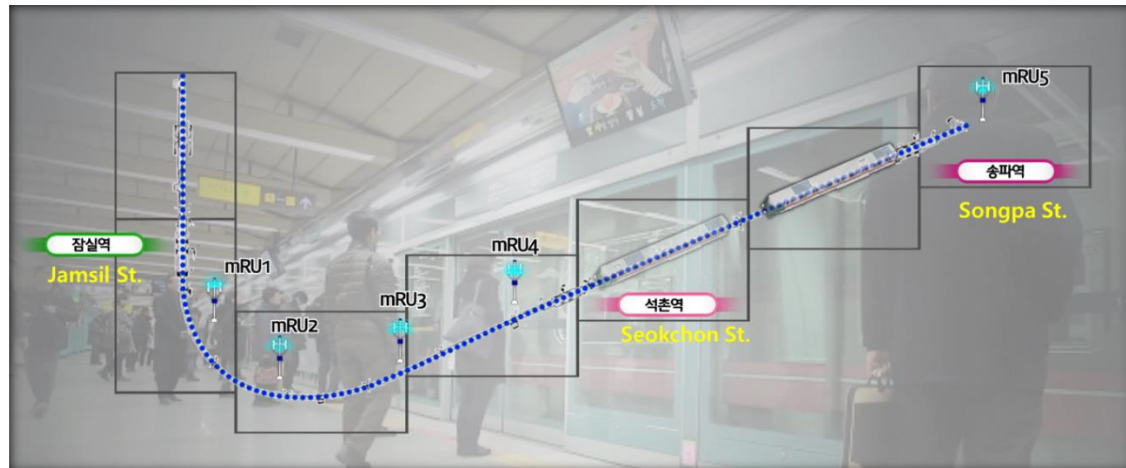


Figure 41 Seoul subway Line 8 path for a field trial



Figure 42 Picture of installed mRU

An mTE was installed in the engine room of the running train just behind the front window. If the mTE approaches the Jamsil St., it starts a random access to attach to the mNB. As the train runs through the route in the figure, the mTE receives and transmits signals from/to the mRUs on the nearest mRUs. When it passes the mRU, it carries out the handover procedure to connect to the next cell until it pass through the last mRU. Figure 43 illustrates a captured performance monitoring display that includes 64QAM constellation, frequency and time domain impulse responses and downlink and uplink data throughput. The green line (bottom) shows downlink data throughput. It keeps maintaining 1.25 Gbps of data rate most time. Four drop points indicate handover regions. In this field trial, the critical functionalities like handover and data throughput have been proven.



Title: Deliverable D3.5: mmWave backhauling & fronthauling platform

Date: 05-06-2017

Status: Final

Security: Public

Version: V1.01



Figure 43 Measured performance of the MHN system in a field trial

6 Conclusion

Final performance studies and measurement to be reported on D3.6 M22

References

- [1] 5GCHAMPION report "Preliminary 5GCHAMPION architecture specifications (IR2.1)," 2016.
- [2] J. Kim and I. G. Kim, "Distributed antenna system-based millimeter-wave mobile broadband communication system for high speed trains," 2013 International Conference on ICT Convergence (ICTC), Jeju, 2013, pp. 218-222.
- [3] S. W. Choi, H. Chung, J. Kim, J. Ahn, and I. Kim, "Mobile Hotspot Network System for High-Speed Railway Communications Using Millimeter Waves," ETRI Journal, vol. 38, no. 6, pp. 1042-1051, December 2016.
- [4] 3GPP TR 38.913, "Study on Scenarios and Requirements for Next Generation Access Technologies," 2016.
- [5] Destino Giuseppe etc, submitted, "Multiple antenna techniques for device pairing of a mmWave high capacity backhaul system"
- [6] 5GCHAMPION report "5GCHAMPION architecture specifications (IR2.1)," 2016.
- [7] 5GCHAMPION report "5GCHAMPION Front-end design (D3.1)" 2017.
- [8] 5GCHAMPION report "5GCHAMPION Electronically reconfigurable antenna arrays for backhauling & fronthauling (D3.2)," 2017.

The information contained in this document is the property of the contractors. It cannot be reproduced or transmitted to thirds without the authorization of the contractors.



Title: Deliverable D3.5: mmWave backhauling & fronthauling platform

Date: 05-06-2017

Status: Final

Security: Public

Version: V1.01

- [9] 5GCHAMPION report “5GCHAMPION Architecture, API- and interface (D2.1),” 2017.
[10] 5GCHAMPION report “5GCHAMPION Key Performance Indicator and use cases (D2.2),” 2017.
[11] 5GCHAMPION report “5GCHAMPION “Algorithms for backhauling & fronthauling (D3.4),” 2017